EFFECT OF DRILLING PARAMETERS ON DRILLING TEMPERATURE AND FORCE OF ULTRA-HIGH STRENGTH STEEL

by

Hui ZHANG[a], Changsheng GUO[b], and Changming ZHANG[b*]

[a] School of Materials Science and Engineering, Shaanxi University of Technology, Hanzhong, China
[b] School of Mechanical Engineering, Shaanxi University of Technology, Hanzhong, China

Original scientific paper
https://doi.org/10.2298/TSCI181125146Z

Aiming at 300M hard-to-machine material, the effects of different drilling parameters (spindle speed, n, feed, f, bit diameter, d) on drilling temperature, torque and axial force were analyzed and studied by orthogonal test method. The prediction models of drilling temperature, torque, and drilling axial force are constructed. The results show that the cutting temperature and stress are mainly distributed on the cross edge of the bit in the initial stage of 300 m steel drilling. With the continuous drilling process of 300M hard-to-machine materials, the cutting temperature and stress generated gradually transfer to the main cutting edge of the bit and extend along the main cutting edge. With the increase of bit diameter, the cutting axial force, torque and cutting temperature decrease, but the cutting axial force, torque and cutting temperature decrease. With the increase of spindle speed and feed, the cutting temperature is increasing. According to the results of orthogonal experiment, the cutting axial force is established by least square method. The predictive models of force, torque, and cutting temperature are validated by the experimental model coefficients and model coefficients. The results show that feed, f, has the greatest influence on cutting axial force, torque, and cutting temperature.

Key words: *300M steel, drilling, cutting temperature, axial force, torque*

Introduction

Hole processing plays an important role in mechanical processing. According to statistics, hole processing time accounts for 50~70% in mechanical processing, and 70% of chips are produced. Drilling is the main method of hole processing. Drilling is a semi-enclosed process, the processing environment is relatively bad, a large amount of cutting heat is concentrated near the cutting edge, it is difficult to discharge, cutting temperature is high, and tool wear is serious [1-3].

The 300M steel (40CrNi2Si2Mova) is a kind of ultra-high strength steel, a kind of medium carbon low alloy steel, which has the characteristics of high strength, high hardness and poor thermal conductivity. At present, 300M difficult-to-machine material has become the world's highest strength, the best comprehensive performance, and is the most widely used steel in aircraft landing gear [4-6]. As an aerospace difficult-to-machine material, it causes tool wear rapidly and machining performance is poor in the process of material removal due to its high strength, high fracture toughness and large transverse plasticity [7-9]. It mainly includes short tool life, large residual stress on the workpiece surface, large cutting force and high temperature in the cutting zone during the cutting process [10]. Aircraft landing gear is key force structural

* Corresponding author, e-mail: zhangchangmingsx@126.com

parts for aviation, and quality of its processing surface is critical to their service performance and life [11, 12]. While the greatest effect on service performance of the parts is the physical level of machined surface quality, which is more significantly affected by the microstructure evolution and cutting heat [13].

At present, scholars of various countries have done many researches on cutting force and surface roughness when cutting difficult to machine materials, and mainly focusing on the milling and turning performance, while the research on drilling performance of 300M steel is relatively less. Zhang *et al.* [14] established an empirical formula for cutting force of 300M steel by orthogonal test method, and analyzed the influence of various parameters using cutting force's maximum value. Wyen and Wegener [15] by means of orthogonal tests conducted on TC18 titanium alloy with the impact of different cemented carbide tool geometric parameters on milling force and surface integrity in milling process. Ozel and Zeren [16] obtained optimized parameters of the Johnson-Cook (J-C) equation of 300M steel, which based on its cutting experimental data, genetic algorithm and correctness of proposed method, is verified by applying it to the orthogonal cutting simulation in Advant-Edge FEM software. Du *et al.* [17] have been studied the softening mechanism of GH4169, a commonly used in aerospace industry products, to the surface degenerating layer during grinding. Li *et al.* [18] conducted high-speed milling of GH4169, and used orthogonal test method to determine empirical model of the machined surface roughness. Wang *et al.* [19] analyzed surface roughness and cutting force in high-speed milling process of titanium alloy Ti6Al4V. Umbrello [20] reported the changes of the microhardness and microstructure of the surface roughness with the cutting parameters when he was processed under dry cutting conditions for inconel 718. Fetecau *et al.* [21] found that surface roughness improved significantly with increasing the spindle speed gradually under different machining conditions. Suet and Zhang [22] established an empirical model to analyze milling parameters affecting cutting force, and proposed out that cutting force is an important factor affecting morphology of workpiece. Azizi *et al.* [23] concluded that the change of cutting force and surface roughness is closely related to milling parameters and workpiece hardness through studying AISI 52100 steel. Liu and Li [24] made a study on the hot deformation behavior and microstructure evolution of 300M steel by experiments, and analyzed the stress-strain curves under various temperatures. Chen *et al.* [25] observed metallographic structure under various deformation conditions, which was made from high temperature deformation compression experiments on 300M steel, and established its thermal deformation equation. Sun and Guo [26] found that the residual stress in direction of machining surface feed and cutting were both compressive stresses when Ti-6Al-4V was reverse-milled, and its absolute values increased with increasing of the cutting speed, while decreased with increasing of the feed rate. Varela *et al.* [27] analyzed the effect of different tool geometries and processing parameters on residual stress and surface roughness at machining 300M steel. Liu *et al.* [28] based on the orthogonal test method, the empirical formula of tool life for high-speed turning of 300M steel with Al_2O_3-based ceramic tools was established. Liu *et al.* [29] established the forecasting model of the temperature field of the workpiece end of the orthogonal Turning-Milling complex difficult-to-machine material; and the model was verified by the orthogonal Turning-Milling test of 300M steel. Xie *et al.* [30] milling 300M steel with coated cutter was studied experimentally, and the Mechanism of tool wears in milling 300M steel was analyzed. Chen *et al.* [31] studied the hot deformation behavior and microstructure evolution of 300M steel through experiments, and analyzed the stress-strain curves at various temperatures. Liu *et al.* [32] performed a high temperature thermal deformation compression test on 300M steel, observed the metallographic structure under various deformation conditions.

In the process of cutting, cutting force and cutting temperature can be predicted by finite element modelling technology, which provides a valid theoretical support for subsequent processing experiments [33]. In this paper, the third Wave AdvantEdge FEM software is used to build a 3-D simulation model, and the effects of different drilling parameters on the drilling axial force, torque and drilling temperature during the drilling processing of 300M steel are analyzed, which provides parameters for the optimization of drilling of 300M steel.

Establish simulation models

This paper chooses the 3-D drilling simulation module of AdvantEdge FEM simulation software to simulate the drilling process of 300M steel, and predicts the changes of drilling axial force, torque and drilling temperature during the processing of drilling. The workpiece material is 300M steel (550 Bhn), the chemical composition is shown in tab. 1, the mechanical properties are shown in tab. 2, and the tool material is CBN. Considering the interaction between cutting parameters, the orthogonal test method is used to simulate the drilling axial force, torque and drilling temperature. The level of experimental factors is shown in tab. 3.

Table 1. Chemical constitution of 300M Steel [%]

C	Mn	Si	Cr	Ni	Mo	V	P	S	Fe
0.43	0.775	1.625	0.825	1.825	0.375	0.05	0.035	0.04	Bal.

Table 2. Mechanical properties of 300M steel

Tensile strength, σ_b [MPa]	Yield strength, $\sigma_{0.2}$ [MPa]	Reduction of area, ψ [%]	Elongation, δ [%]	Elastic modulus, E [GPa]
1970	1655	34%	9.5%	199

Table 3. The 300M test factor level table

Level	d [mm]	n [rpm]	f [mmr^{-1}]
1	6	600	0.04
2	10	1000	0.08
3	14	1400	0.12

Simulation results analysis

The test schemes and results of drilling axial force, torque and drilling temperature are shown in tab. 4.

Table 4. Test program and test results

Number	d [mm]	n [rpm]	f [mmr^{-1}]	F [N]	M [Nm]	T [°C]
1	6	600	0.04	478.32	0.1	69.44
2	6	1000	0.08	1244.54	0.26	170.96
3	6	1400	0.12	1458.50	0.35	263.87
4	10	600	0.08	1012.27	0.22	104.04
5	10	1000	0.12	1153.22	0.31	170.02
6	10	1400	0.04	490.99	0.11	143.94
7	14	600	0.12	1140.92	0.24	105.89
8	14	1000	0.04	400.05	0.08	38.51
9	14	1400	0.08	957.53	0.19	195.33

Analysis of cutting stress and cutting temperature of drill bit

Figure 1 shows the distribution of cutting stress and cutting temperature. As shown in fig. 1(a), the cutting temperature is mainly distributed on the cross edge and the main cutting edge of the bit. This is because in the process of drilling, the cross edge of the bit first contacts with the workpiece, and through extrusion produces axial force to cut the workpiece. The workpiece is formed chips due to extrusion deformation, and then separates from the workpiece. Therefore, in the initial stage of drilling, the temperature of the cross edge of the bit is higher. With the continuous drilling process, when the main cutting edge begins to cut, the cutting heat gradually diffuses to the main cutting edge, and the temperature field range gradually enlarges. As shown in the figure, the maximum temperature on the main cutting edge is 353.9 °C. This is because most of the heat in cutting is carried off by chips during cutting, and the chips temperature is higher than that of the workpiece and the cutting tool. As can be seen from fig. 1(b), cutting stress mainly distributes on the cross and main edges of the bit. When drilling begins, the maximum stress appears at the contact part between the cross edge and the workpiece, with a value of 1000 MPa. When the main cutting edge of the bit begins to enter the part cutting, the maximum stress moves along the main cutting edge to the contact part between the main cutting edge and the work piece, and along the main cutting edge. The cutting edge of the bit gradually expands and keeps the maximum stress in the main cutting process basically the same.

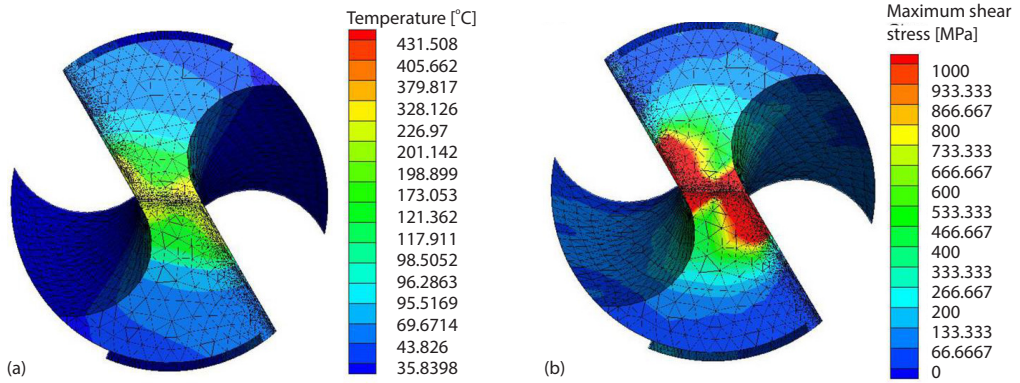

Figure 1. Distribution of cutting stress and cutting temperature

Visual analysis of results

Figure 2 is an intuitive analysis of the results. As shown in fig. 2(a) that with the increase of bit diameter, the drilling axial force, torque and cutting temperature decrease. This is because as the diameter of the bit increases, the friction area of the bit increases, and the specific heat capacity increases, so when the diameter of the bit increases, the drilling temperature decreases, but the influence is small. As shown in fig. 2(b), with the increase of spindle speed, drilling axial force, torque and cutting temperature also increase. With the increase of spindle speed, the feed speed per unit time of drill bit increases. Because the elastic modulus of 300M steel is small, the rebound resistance of the axial direction and the hole wall increases with the increase of the bit feed speed, which correspondingly increases the drilling axial force and the drilling torque. When the spindle speed increases, the feed is smaller, so the friction distance between the drill bit and the drilled surface is increased, and the heat is increased. Therefore, the higher the spindle speed is, the higher the drilling temperature is. From fig. 2(c), it can be seen

that the drilling axial force, torque and cutting temperature increase with the increase of the feed. The reason for this trend is that the increase of feed makes the cutting thickness and cutting force increase, and the corresponding drilling axial force and torque increase. When feed increases, the friction distance in unit time becomes shorter and the heat production decreases, but the increase of metal material cutting deformation and total heat production in unit time increases, so the larger feed, the drilling. The higher the cutting temperature.

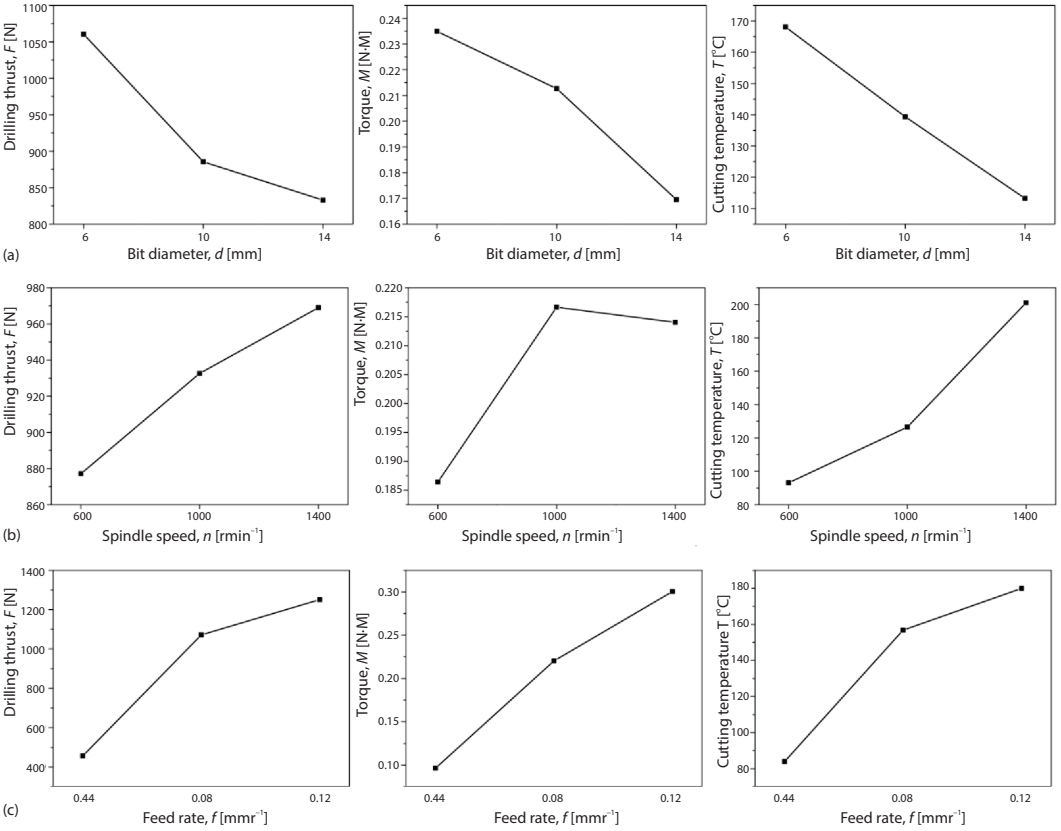

Figure 2. Visual analysis of results

Model establishment

Model establishment

According to the basic metal cutting theory, the prediction models of drilling axial force, torque and drilling temperature are constructed by least square method:

$$\begin{cases} F = K_{F1} d^{b_1} n^{b_2} f^{b_3} \\ M = K_{F2} d^{b_1} n^{b_2} f^{b_3} \\ T = K_{F3} d^{b_1} n^{b_2} f^{b_3} \end{cases} \tag{1}$$

where K_F is the correction coefficient established by the processing material and cutting conditions, d – the diameter of bit, n – the spindle speed, f – the feed, and b_1, b_2 and b_3 are the indices

of each variable to be established. Under drilling conditions, the prediction models of drilling axial force, torque and drilling temperature are:

$$\begin{cases} F = 10^{4.032} d^{-0.270} n^{0.080} f^{0.949} \\ M = 10^{0.442} d^{-0.338} n^{0.117} f^{1.049} \\ T = 10^{0.984} d^{-0.506} n^{0.841} f^{0.794} \end{cases} \tag{0}$$

It can be observed from the equation that the cutting axial force, torque and cutting temperature increase with the increase of spindle speed and feed, and decrease with the increase of bit diameter.

Prediction model significance test

The prediction model significance was verified by F distribution test. The significant level of $\alpha = 0.05$, $F_{0.05}(p, n\text{-}p\text{-}1) = F_{0.05}(3, 5) = 5.41$. From tab. 5, it can be seen that F value is far greater than $F_{0.05}$ value, and the established prediction model is significant.

Table 5. Prediction model significance analysis

Stem	Squeras	Freedom	Mean squares	$F_{0.05}$
F	0.331	3	0.110	27.478
M	0.411	3	0.137	64.253
T	0.419	3	0.140	6.855

Coefficient of model significance test

The model coefficients' validity is verified by t-test. Significant levels were $\alpha = 0.05$, $t_{(\alpha/2)}(n\text{-}p\text{-}1) = t_{0.025}(5) = 2.571$. As shown in tab. 6, the influence of feed on cutting axial force, torque and cutting temperature is the most significant, followed by spindle speed and bit diameter.

Table 6. Significance analysis of prediction model

Stem	β_1	β_2	β_3	$t_{0.025}$
	$\lvert d \rvert$	$\lvert n \rvert$	$\lvert f \rvert$	
F	–1.935	0.574	8.852	$\beta_3 > 2.201 > \beta_2 > \beta_1$
M	–3.324	1.147	13.431	$\beta_3 > 2.201 > \beta_2 > \beta_1$
T	–1.609	2.675	3.289	$\beta_3 > \beta_2 > 2.201 > \beta_1$

Conclusion

Through the finite element simulation study of the drilling process of 300M difficult-to-cut ultra-high strength steel, the influence of different cutting parameters on the drilling axial force, torque and cutting temperature is studied by using orthogonal test method and range analysis method. The following conclusions are drawn: with the increase of drill diameter, the cutting axial force, torque and cutting temperature decrease, while the cutting axial force, torque and cutting temperature increase with the increase of spindle speed and feed. In the initial stage of drilling 300M steel, the cutting temperature and cutting stress mainly distribute on the cross edge of the bit. With the continuous drilling process, the cutting hot and cutting temperature increase. The cutting stress gradually shifts to the main cutting edge and expands

along the drill main cutting edge. According to the results of orthogonal test, a prediction model including cutting axial force, torque and cutting temperature was built by least square method. The validity of the model is verified by the test of model and model coefficients, and the results are close to the three cutting parameters. The influence of cutting parameters on cutting axial force, torque and cutting temperature is the most significant, followed by spindle speed and bit diameter.

Acknowledgment

This work was funded by the China National Natural Science Foundation (Grant No. 51505268).

References

[1] Ucun, I., The 3-D fFinite Element Modelling of Drilling Process of Al7075-T6 Alloy and Experimental Validation, *Journal of Mechanical Science and Technology*, *30* (2016), 4, pp. 1843-1850
[2] Nam, *et al*., Machinability of Titanium Alloy (Ti-6Al-4V) in Environmentally-Friendly Micro-Drilling Process with Nanofluid Minimum Quantity Lubrication Using Nanodiamond Particles, *International Journal of Precision Engineering and Manufacturing-Green Technology*, *5* (2018), 1, pp. 29-35
[3] Polli, *et al*., Effects of Process Parameters and Drill Point Geometry in Deep Drilling of SAE 4144M under MQL, *Journal of the Brazilian Society of Mechanical Sciences and Engineering*, *40* (2018), Mar., 137
[4] Figueroa, D., Robinson, M. J., Hydrogen Transport and Embrittlement in 300M and AerMet100 Ultra High Strength Steels, *Corrosion Science*, *52* (2010), 5, pp. 1593-1602
[5] Pistochini, T. E., Hill, M. R., Effect of Laser Peening on Fatigue Performance in 300M Steel, *Fatigue and Fracture of Engineering Materials and Structures*, *34* (2011), 7, pp. 521-533
[6] Liu, *et al*., Effect of Dilution and Macrosegregation on Corrosion Resistance of Laser Clad AerMet100 Steel Coating on 300M Steel Substrate, *Surface and Coatings Technology*, *325* (2017), Sept., pp. 352-359
[7] Zheng, G., *et al*., Effect of Cutting Parameters on Wear Behavior of Coated Tool and Surface Roughness in High-Speed Turning of 300M, *Journal Measurement*, *125* (2018), Sept., pp. 99-108
[8] Lee, E. U., Waldman, J., Corrosion of Aircraft Landing Gear Steels, *Naval Engineers Journal*, *106* (2010), 6, pp. 77-83
[9] Sen, L., *et al*., An Investigation of Workpiece Temperature Variation in end Milling Considering Flank Rubbing Effect, *International Journal of Machine Tools and Manufacture*, *73* (2013), 7, pp. 71-86
[10] Remes, H., *et al*., Influence of Surface Integrity on the Fatigue Strength of High-Strength Steels, *Journal of Constructional Steel Research*, *89* (2013), 5, pp.21-29
[11] Hu, C. Y., *et al*., Failure Analysis of Rotating Shaft in Main Undercarriage, *ActaAeronautica et Astronautica Sinica*, *35* (2014), 2, pp. 461-468
[12] Yang, S., *et al*., Workpiece Temperature Analysis and Its Impact on Machined Surface Quality of Ultra-High Strength Steel in end Milling, *Acta Aeronautica et Astronautica Sinica*, *36* (2015), 5, pp. 1722-1732
[13] Zhang, H. P., *et al*., Milling Force Modelling and Experimental Research of 300M Ultra High Strength Steel, *Materials Science Forum*, *800-801* (2014), July, pp. 53-60
[14] Wyen, C. F., Wegener, K., Influence of Cutting Edge Radius on Cutting Forces in Machining Titanium, CIRP Annals, *Manufacturing Technology*, *59* (2010), 1, pp. 93-96
[15] Ozel, T., Zeren, E., A Methodology to Determine Work Material Flow Stress and Tool-Chip Interfacial Friction Properties by Using Analysis of Machining, *Waste Management*, *26* (2006), 1, 106
[16] Du, S. U., *et al*., Softening Mechanism of Grinding Surface Metamorphic Layer of GH4169DA, *Acta Aeronautica et Astronautica Sinica*, *35* (2014), 5, pp. 1446-1451
[17] Li, X., *et al*., Influences of Milling and Grinding on Machined Surface Roughness and Fatigue Behavior of GH4169 Superalloy Workpieces, *Chinese Journal of Aeronautics*, *31* (2018), 6, pp. 1399-1405
[18] Wang, F. Z., *et al*., Cutting Forces and Surface Roughness in High-Speed end Milling of Ti6Al4V, *Key Engineering Materials*, *589-590* (2014), Oct., pp.76-81
[19] Umbrello, D., Investigation of Surface Integrity in Dry Machining of Inconel 718, *International Journal of Advanced Manufacturing Technology*, *69* (2013), 9-12, pp. 2183-2190
[20] Fetecau, C., *et al*., Machining and Surface Integrity of Polymeric Materials, *International Journal of Material Forming*, *1* (2008), 1, pp. 515-518

[21] Suet, T., Zhang, G., Study of Cutting Force in Ultra-Precision Raster Milling of V-Groove, *International Journal of Advanced Manufacturing Technology*, *75* (2014), 5-8, pp. 967-978
[22] Azizi, M. W., *et al*., Surface Roughness and Cutting Forces Modelling for Optimization of Machining Condition in Finish Hard Turning of AISI 52100 Steel, *Journal for Manufacturing Science and Production*, *26* (2015), 3, pp. 4105-4114
[23] Liu, Y. G., Li, M. Q., Study on the Dynamic Recrystallization of Austenite in the Isothermal Compression of 300M Steel, *Materials Science Forum*, *773-774* (2013), Nov., pp. 39-46
[24] Chen, X. M., *et al*., Dynamic Recrystallization Behavior of a Typical Nickel-Based Superalloy during Hot Deformation, *Materials and Design*, *57* (2014), 5, pp. 568-577
[25] Sun, J., Guo, Y. B., A Comprehensive Experimental Study on Surface Integrity by end Milling Ti-6Al-4V, *Journal of Materials Processing Tech.*, *209* (2009), 8, pp. 4036-4042
[26] Varela, P. I., *et al*., Surface Integrity in Hard Machining of 300 M Steel: Effect of Cutting-Edge Geometry on Machining Induced Residual Stresses, *Procedia Cirp*, *13* (2014), Dec., pp.288-293
[27] Liu, W. M., *et al*., Wear Mechanisms of Al_2O_3-Based Ceramic Cutting Tool in High Speed Turning of 300M Ultra High Strength Steel, *Journal Tribology*, *36* (2011), 6, pp. 564-568
[28] Liu, Y. Z., *et al*., Experimental Research of Workpiece Temperature in Orthogonal Turn-Milling Compound Machining, *Journal Advanced Materials Research*, *887-888* (2014), Feb., pp. 1184-1190
[29] Xie, J. X., *et al*., Study of Tool Materials Rapid Selection in Cutting 300M Steel, *Journal Advanced Materials Research, 472-475* (2012), Feb., pp. 986-990
[30] Chen, X. M., *et al.*, Dynamic Recrystallization Behavior of a Typical Nickel-Based Superalloy during Hot Deformation, *Journal Materials and Design*, *57* (2014), May, pp. 568-577
[31] Liu, Y. G., *et al*., The Study on Kinetics of Static Recrystallization in the Two-Stage Isothermal Compression of 300M Steel, *Journal Computational Materials Science*, *84* (2014), Mar., pp. 115-121
[32] Li, H. Z., Wu, B ., Development of a Hybrid Cutting Force Model for Micromilling of Brass, *International Journal of Mechanical Sciences*, *115-116* (2016), Sept., pp. 586-595

Paper submitted: November 25, 2018
Paper revised: January 20, 2019
Paper accepted: January 30, 2019